ELSEVIER

Catalysis Today 74 (2002) 23–35

CATALYSIS TODAY

www.elsevier.com/locate/cattod

Macro-kinetics of biphasic hydroformylation of 1-dodecene catalyzed by water-soluble rhodium complex

Yongqiang Zhang[1], Zai-Sha Mao*, Jiayong Chen

Institute of Chemical Metallurgy, Chinese Academy of Sciences, Beijing 100080, China

Abstract

Hydroformylation of 1-dodecene was studied in a biphasic system using water-soluble rhodium complex, RhCl(CO)(TPPTS)$_2$ (TPPTS: $P(m\text{-}C_6H_4SO_3Na)_3$), as catalyst in the presence of cetyl trimethyl ammonium bromide (CTAB) as surfactant to enhance the reaction rate. The reaction was carried out in a batch reactor at pressures from 0.9 to 1.3 MPa and temperatures from 353 to 373 K. An orthogonal experimental design was adopted to study the effects of operating variables on reaction rate, selectivity and normal/isomeric aldehyde ratio. The optimal reaction conditions were derived by margin and variance analyses. The analysis of mass transfer indicates that in some cases the gas–liquid mass transfer rate is still a controlling factor. An empirical kinetic equation was developed after correcting the effect of mass transfer. Combining mechanisms of homogeneous hydroformylation with interfacial reaction of biphasic hydroformylation, a semi-empirical kinetic equation was also obtained. © 2002 Elsevier Science B.V. All rights reserved.

Keywords: 1-Dodecene; Hydroformylation; Gas–liquid–liquid system; Reaction engineering; Kinetics; Surfactant

1. Introduction

Hydroformylation of olefins with CO and H_2 is an important commercial process for the production of aldehydes and alcohols. Homogeneous catalysts such as $Co_2(CO)_8$ and $HRh(CO)(PPh_3)_3$ are widely used for this reaction. A striking drawback of this process is the difficulty in separating and recovering catalysts from the mixture of reaction products and solvent, especially for expensive catalysts made from noble metals. Therefore, it is preferred to use heterogeneous catalysts to overcome this difficulty. The biphasic (aqueous–organic) hydroformylation of propylene has been successfully commercialized to produce butyraldehyde using water-soluble rhodium complexes as the catalyst. This technique provides a simple method for the separation of the reaction products in the organic phase from the catalyst in the aqueous phase immediately after the reaction [1,2]. When it is applied to the hydroformylation of higher olefins, the reaction rate becomes very low for practical insolubility of higher olefins in the aqueous phase [3–6]. However, the addition of cosolvent or surfactant enhances the reaction rate [3–7].

The biphasic hydroformylation of higher olefins occurs in a typical gas–liquid–liquid system. The nature of new catalytic complexes and ligands will certainly determine the intrinsic activity and selectivity of such catalysts. However, an equally important factor is the effectiveness of contact between gas and liquid reactants and the catalyst contained in certain phase, as being demonstrated in the case of propylene hydroformylation in a gas–liquid system [8]. It largely

---

* Corresponding author.

[1] Present address: Research Institute of Petroleum Processing, SINOPEC, Beijing 100083, China.

0920-5861/02/$ – see front matter © 2002 Elsevier Science B.V. All rights reserved.
PII: S0920-5861(01)00527-2

depends on the hydrodynamics of gas–liquid–liquid dispersion, interphase mass transfer, solubility and phase equilibrium, interfacial properties, as well as the intrinsic kinetics of the reaction concerned. Hence, a comprehensive investigation of macro-kinetics, which is incorporated with the interaction between the mass transfer and the reaction rate, is of great importance.

Nomenclature

C	concentration ($\mathrm{kmol\,m^{-3}}$)
D	diffusivity ($\mathrm{m^2\,s^{-1}}$)
H	Henry constant (MPa)
H_1/H_2	ratio of distance between stirrer and reactor bottom to liquid height
k	kinetic rate constant
k_La	gas–liquid volumetric mass transfer coefficient ($\mathrm{s^{-1}}$)
K	equilibrium constant
m	partition coefficient ($\mathrm{kg\,kmol^{-1}}$)
M	molecular weight
n	stirrer speed ($\mathrm{s^{-1}}$)
N	gas–liquid mass transfer rate ($\mathrm{kmol\,m^{-3}\,s^{-1}}$)
p	pressure (MPa)
p^*	equilibrium partial pressure with dissolved solute (MPa)
[P]/[Rh]	ligand/catalyst molar ratio
R	reaction rate ($\mathrm{kmol\,m^{-3}\,min^{-1}}$)
R_0	initial reaction rate ($\mathrm{kmol\,m^{-3}\,min^{-1}}$)
R_{ni}	normal/isomeric mole ratio
TOF	turnover frequency ($\mathrm{mol\,mol^{-1}\,s^{-1}}$)
$V_{\mathrm{O}}/V_{\mathrm{W}}$	organic/aqueous volume ratio
W_{CTAB}	weight percentage of CTAB in water (%)
W_{d}	weight percentage of hydrogenation product (%)
X	reaction conversion (%)

Greek letter

ρ	density ($\mathrm{kg\,m^{-3}}$)

Superscript

$*$	equilibrium

Subscripts

cat	catalyst
CO	carbon monoxide
d1	1-dodecene
G	gas phase
H_2	hydrogen
I	liquid–liquid interface
O	organic phase
S	solvent
T	total
W	aqueous phase

Recently, Deshpande et al. [9] studied the kinetics of biphasic hydroformylation of 1-octene using $[RhCl(1,5\text{-}COD)]_2$/TPPTS as catalyst with the addition of ethanol as cosolvent. The cosolvent greatly increased the solubility of 1-octene in water, resulted in significant enhancement of the hydroformylation reaction occurring in the aqueous phase.

Chen et al. [4] have investigated the biphasic hydroformylation of 1-dodecene using $RhCl(CO)(TPPTS)_2$/TPPTS as catalyst in the presence of surfactant cetyl trimethyl ammonium bromide (CTAB) under atmospheric pressure. The molar ratio of normal to branched aldehyde in the reaction product is rather high (up to 20) and the reaction rate was also significantly enhanced by the surfactant. It was believed that the reaction took place at the liquid–liquid interface [7,10], which is obviously different from biphasic hydroformylation with cosolvent.

The chemical kinetics is the basis for modeling and design of chemical reactors. As for biphasic hydroformylation, the mass transfer behavior in the reactor is of equal importance to the macroscopic chemical kinetics. The macro-kinetics, which contains the interaction of mass transfer and chemical reaction under practical technological conditions, provides the necessary basis for modeling and designing biphasic hydroformylation reactors. Thus, the investigation of the macro-kinetics of biphasic hydroformylation is of great significance.

Based on the works of Chen et al. [4,10], this paper presents a detailed macro-kinetic study of biphasic hydroformylation of 1-dodecene with $RhCl(CO)(TPPTS)_2$/TPPTS as catalyst in the presence of surfactant CTAB under practical operating conditions. The optimal operating conditions are suggested and the mechanism of biphasic hydroformylation is discussed.

Table 1
Experimental design of kinetic experiments with the orthogonal table $L_{18}(2^1 \times 3^7)$

Number	Factor							
	[P]/[Rh]	C_{d1} (kmol m^{-3})	y_{H_2}/y_{CO}	p (MPa)	C_{cat} ($\times 10^3$ kmol m^{-3})	T (K)	V_O/V_W	W_{CTAB} (%)
1	1 (18)	1 (4.4)[a]	1 (4/1)	1 (0.9)	1 (0.75)	1 (353)	1 (3/7)	1 (0.4)
2	1	1	2 (1/1)	2 (1.1)	2 (1.0)	2 (363)	2 (1/1)	2 (0.3)
3	1	1	3 (1/4)	3 (1.3)	3 (1.5)	3 (373)	3 (7/3)	3 (0.35)
4	1	2 (2.2)	1	1	2	2	3	3
5	1	2	2	2	3	3	1	1
6	1	2	3	3	1	1	2	2
7	1	3 (1.6)	1	2	1	3	2	3
8	1	3	2	3	2	1	3	1
9	1	3	3	1	3	2	1	2
10	2 (30)	1	1	3	3	2	2	1
11	2	1	2	1	1	3	3	2
12	2	1	3	2	2	1	1	3
13	2	2	1	2	3	1	3	2
14	2	2	2	3	1	2	1	3
15	2	2	3	1	2	3	2	1
16	2	3	1	3	2	3	1	2
17	2	3	2	1	3	1	2	3
18	2	3	3	2	1	2	3	1

[a] Parameter value at certain level is bracketed.

2. Experimental

Hydroformylation of 1-dodecene was carried out in a stirred stainless steel autoclave with a capacity of 500 ml. This reactor was designed to withstand pressure of 10 MPa and temperature up to 200 °C and equipped with an automatic temperature control system consisting of an external electrical heating jacket and an internal water cooling coil. The temperature change could be controlled within ±1 K and the pressure maintained constant within ±5 kPa. The reactor is also equipped with a sampling system and a Rushton turbine stirrer.

The yellowish solid catalyst ($RhCl(CO)(TPPTS)_2$) and white powder ligand (TPPTS) were provided by Prof. X.J. Li, Sichuan University, China. 1-Dodecene was purchased from Fluka, Switzerland and Aldrich, USA. Syngas (mixture of CO and H_2) was obtained from Beijing Huayuan Chemical Gas Co., China. CTAB was of analytical purity, and the solvent *n*-decane was of chemical purity. Deionized water was used in all experiments.

The experimental conditions for kinetic study were listed in Table 1. In all cases, the total volume of liquids in the reactor was 200 ml. In a typical experimental run, the required catalyst, ligand, deionized water and surfactant were added to the reactor, and then the desired amount of 1-dodecene and *n*-decane were added, following this, the reactor was flushed with nitrogen first, and then with syngas. The reactor was heated to the specified temperature. After that, the syngas was introduced at the desired pressure, which was kept constant during the run. Switching on the stirrer started the reaction, and a liquid sample was withdrawn at the same time. Liquid samples were collected at regular intervals to follow the reaction by gas chromatography.

3. Results and discussion

3.1. Preliminary experiments

To ensure the reaction is in the chemical reaction-controlling region, preliminary experiments were carried out at temperature of 363 K with different stirring speeds. It was observed that the reaction rate was enhanced greatly with the increase of the agitation speed at first and then approached to a constant. However, when the agitation speed was higher than 15 s^{-1}, the

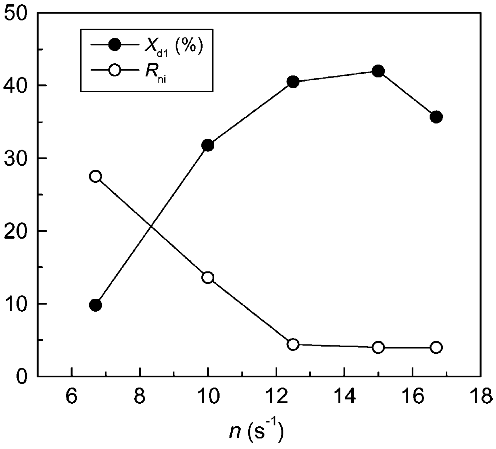

Fig. 1. Plot of X_{d1} and R_{ni} of hydroformylation of 1-dodecene versus stirrer speed (n). Conditions: $p = 1.1\,\mathrm{MPa}$; $y_{H_2}/y_{CO} = 53/47$; $T = 363\,\mathrm{K}$; $C_{cat} = 0.001\,\mathrm{kmol\,m^{-3}}$; [P]/[Rh] = 18; 100 ml 1-dodecene; 100 ml water; $W_{CTAB} = 0.3\%$; 2 h.

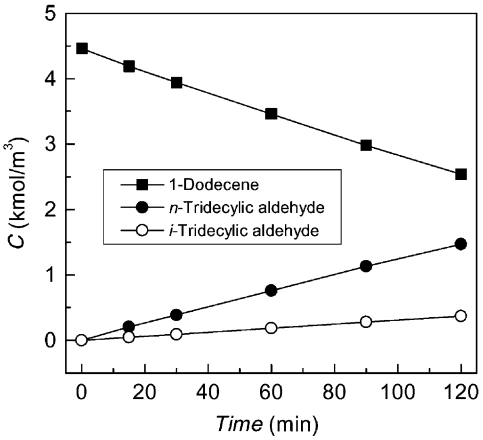

Fig. 2. Typical plot of concentrations of 1-dodecene and tridecylic aldehydes versus reaction time. Conditions: $n = 15\,\mathrm{s^{-1}}$; others are the same as in Fig. 1.

rate decreased as shown in Fig. 1. As reported by Bahrmann and Lappe [5] and Chen et al. [10], the cationic surfactant is able to attract the water-soluble catalyst to the liquid–liquid interface so that the coordination with olefin in the organic phase proceeds more easily. Besides, the presence of CTAB leads to the formation of ordered assembly of micelles in favor of producing more linear aldehyde. These result in higher rate of hydroformylation reaction and higher stereoselectivity to normal aldehyde. Too vigorous stirring rate might promote destruction of such ordered assembly, reduces the reaction rate and then leads to lower ratio of normal/isomeric aldehyde. Therefore, all the subsequent experimental runs were conducted at the fixed agitation speed of $15\,\mathrm{s^{-1}}$.

3.2. *Orthogonal experimental results on macroscopic reaction kinetics*

The biphasic hydroformylation of 1-dodecene is a complicated gas–liquid–liquid three-phase reaction and the reaction rate is influenced by many factors. To conduct an effective experimental investigation, an orthogonal experimental design was adopted to arrange the variables at different levels as listed in Table 1. The effects of the following variables on the reaction were examined: temperature, pressure, the parial pressure ratio of H_2 to CO, concentrations of catalyst, olefin and surfactant, molar ratio of ligand to catalyst, and the volume ratio of organic phase to aqueous phase. The typical concentrations of 1-dodecene and tridecylic aldehydes formed versus the reaction time were plotted in Figs. 2–4. The concentration–time profiles of tridecylic aldehyde were used to determine the reaction rate of the formation of tridecylic aldehyde at the initial time. Using a polynomial function best fitted each concentration–time profile, the

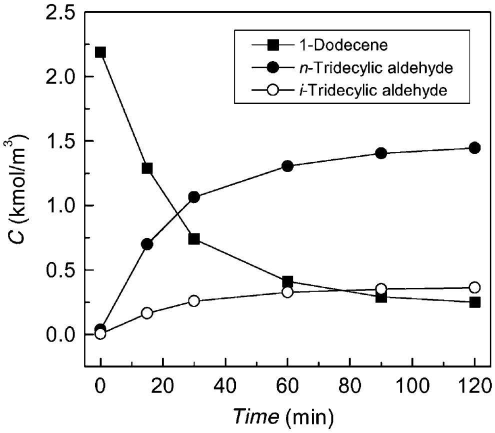

Fig. 3. Typical plot of concentrations of 1-dodecene and tridecylic aldehydes versus reaction time. Conditions: $n = 15\,\mathrm{s^{-1}}$; $p = 1.1\,\mathrm{MPa}$; $y_{H_2}/y_{CO} = 53/47$; $T = 373\,\mathrm{K}$; $C_{cat} = 0.0015\,\mathrm{kmol\,m^{-3}}$; [P]/[Rh] = 18; 30 ml 1-dodecene; 30 ml decane; 140 ml water; $W_{CTAB} = 0.4\%$; 2 h.

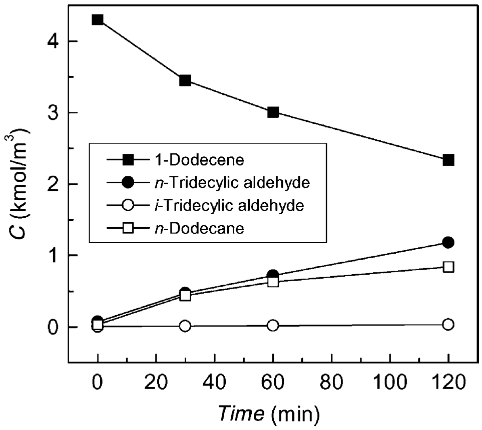

Fig. 4. Typical Plot of concentrations of 1-dodecene and tridecylic aldehydes versus reaction time. Conditions: $n = 15\,\mathrm{s}^{-1}$; $p = 0.9\,\mathrm{MPa}$; $y_{H_2}/y_{CO} = 79.7/20.3$; $T = 353\,\mathrm{K}$; $C_{cat} = 0.00075\,\mathrm{kmol\,m}^{-3}$; [P]/[Rh] = 18; 60 ml 1-dodecene; 140 ml water; $W_{CTAB} = 0.4\%$; 2 h.

reaction rate was obtained from the derivative of the fitted concentration–time curve. The experimental results under the reaction conditions listed in Table 1 were summarized in Table 2.

As given in Table 2, the initial reaction rates vary markedly with different reaction conditions, suggesting that optimization of the reaction conditions for enhanced reaction rate and selectivity be of significant techno-economical importance. From the calculated TOF in the last column of Table 2, it is observed that the TOF of hydroformylation of 1-dodecene with the presence of CTAB may be well above $0.20\,\mathrm{s}^{-1}$, showing quite high catalytic activity of this biphasic system for hydroformylation of 1-dodecene. The TOFs obtained in this study are comparable with that in Chen et al. [11].

3.3. Margin analysis and variance analysis

3.3.1. Margin analysis

The margin analysis was exploited to determine the qualitative influence of reaction conditions on the reaction indexes (initial reaction rate: R_0; molar ratio of normal/isomeric aldehyde: R_{ni}; weight percentage of hydrogenation product: W_d). For convenience and accuracy of qualitative comparison, the initial rate of reaction was calculated by plotting the concentration of tridecylic aldehyde as a function of time in the region with the conversion of 1-dodecene below 15%. The larger the margin, the more important is the factor to the index. As shown in Table 3, the most important variable to R_0

Table 2
Experimental results on macro-kinetics of hydroformylation of 1-dodecene

Number	R_0 (kmol m^{-3} min^{-1})[a]	r_0 (kmol m^{-3} min^{-1})[b]	R_{ni}	W_d (%)	TOF (s^{-1})
1	0.01356	0.00407	36.5	18.1	0.13
2	0.00765	0.00383	5.6	0.0	0.13
3	0.00678	0.00474	3.8	0.0	0.18
4	0.00118	0.00082	3.8	1.90	0.05
5	0.05492	0.01648	4.0	0.0	0.26
6	0.00271	0.00136	3.1	0.0	0.06
7	0.00772	0.00386	10.4	2.43	0.13
8	0.00185	0.00130	4.2	0.0	0.07
9	0.01156	0.00347	4.1	0.0	0.06
10	0.00927	0.00464	38.7	7.76	0.10
11	0.00144	0.00101	4.9	0.0	0.07
12	0.01034	0.00310	3.8	0.0	0.07
13	0.00070	0.00049	10.5	2.07	0.02
14	0.02241	0.00672	4.1	0.0	0.21
15	0.00894	0.00447	3.9	0.0	0.15
16	0.03024	0.00907	11.2	4.86	0.22
17	0.00256	0.00128	6.8	0.0	0.03
18	0.00276	0.00193	4.0	0.0	0.14

[a] R_0: initial reaction rate calculated based on organic phase volume.

[b] r_0: initial reaction rate calculated based on the total liquid volume.

Table 3
The relative importance of variables to indexes of hydroformylation[a]

Index	Important	⟶							Less important
R_0	Factor	V_o/V_W	T	y_{H_2}/y_{CO}	p	C_{d1}	W_{CTAB}	C_{cat}	[P]/[Rh]
	Level	3/7	373	1/1	1.1	2.2	0.4%	0.0015	18
R_{ni}	Factor	y_{H_2}/y_{CO}	C_{d1}	W_{CTAB}	C_{cat}	V_O/V_W	p	T	[P]/[Rh]
	Level	4/1	4.4	0.4%	0.0015	1/1	1.3	353	30
W_d	Factor	y_{H_2}/y_{CO}	C_{d1}	W_{CTAB}	V_O/V_W	p	C_{cat}	T	[P]/[Rh]
	Level	1/1	2.2	0.35%	7/3	1.1	0.001	373	30

[a] The optimum factors and levels are ordered according to their importance to obtaining the maximum R_0 and R_{ni}, and the minimum W_d.

was volume ratio of organic phase to aqueous phase (V_O/V_W), followed by temperature (T), partial pressure ratio of hydrogen to carbon monoxide (y_{H_2}/y_{CO}), total pressure (p), concentration of 1-dodecene (C_{d1}), weight percentage of surfactant (W_{CTAB}), concentration of catalyst (C_{cat}), and molar ratio of ligand to catalyst ([P]/[Rh]). For R_{ni}, the order was y_{H_2}/y_{CO}, C_{d1}, W_{CTAB}, C_{cat}, V_O/V_W, p, T, and [P]/[Rh]. As for W_d, the sequence was y_{H_2}/y_{CO}, C_{d1}, W_{CTAB}, V_O/V_W, p, C_{cat}, T, and [P]/[Rh]. The importance of a variable changes for different indexes. Meanwhile, the optimum level of a factor was determined by comparing its average index value among different levels, and the optimum level sets of operating conditions for three indexes were also determined as shown in Table 3, which indicated the optimized reaction conditions to reach the maximum R_0 and R_{ni} or the minimum W_d.

3.3.2. Variance analysis

The significance of variable to index was determined by variance analysis of the orthogonal table. The importance of factor to the index is also revealed by its corresponding value of the F-distribution function at a certain level (as shown in Table 4).

The high reaction rate, high normal/isomeric ratio, and less hydrogenated product, are of great importance to the production of aldehyde. Among these, the reaction rate is the most important. Based mainly on the initial reaction rate in appropriate compromise with normal/branched ratio of aldehyde and hydrogenated product, the optimal hydroformylation reaction conditions are as follows:

$$T = 373\,\mathrm{K},\ p = 1.1\,\mathrm{MPa},\ y_{H_2}/y_{CO} = 1/1,$$
$$C_{cat} = 1.5 \times 10^{-3}\,\mathrm{kmol\,m^{-3}},$$
$$[\mathrm{P}]/[\mathrm{Rh}] = 18,\ C_{d1} = 2.2\,\mathrm{kmol\,m^{-3}},\ V_O/V_W = 3/7,$$
$$W_{CTAB} = 0.4\%$$

It is worthwhile to point out some new experimental findings valuable for exploring the mechanism of biphsic hydroformylation of 1-dodecene. From data in Table 2, it is noticed that the high volume ratio of the aqueous/organic phases is in favor of hydroformylation rate. It is now difficult to explain such a striking feature by the reaction mechanism, but light may be shed on this matter by an in-depth understanding of the role of micelles formed when surfactant CTAB is added into the biphasic system. Secondly, it is observed that the normal/*iso*-aldehyde ratio in the product is significantly correlated with the rate of hydrogenation of 1-dodecene, especially when the ratio of partial

Table 4
The relative importance of factors to indexes by variance analysis

Index	Important	⟶						Less important
R_0	V_O/V_W	T	y_{H_2}/y_{CO}	p	W_{CTAB}	C_{d1}	C_{cat}	[P]/[Rh]
R_{ni}	y_{H_2}/y_{CO}	C_{d1}	W_{CTAB}	V_O/V_W	C_{cat}	T	p	[P]/[Rh]
W_d	y_{H_2}/y_{CO}	C_{d1}	W_{CTAB}	V_O/V_W	p	C_{cat}	T	[P]/[Rh]

pressures of H_2:CO is 4:1. The parallelism between the formation of these two species bears certain implication on the hydroformylation mechanism. Further efforts are necessary to get a satisfactory interpretation.

3.4. Macro-kinetic equation

The initial reaction rates were correlated with all variables using the following empirical kinetic model:

$$R_0 = A_0 \exp(A_1/T) p_{H_2}^{A_2} p_{CO}^{A_3} C_{cat}^{A_4} C_{d1}^{A_5} W_{CTAB}^{A_6} \times \left(\frac{[P]}{[Rh]}\right)^{A_7} \left(\frac{V_O}{V_W}\right)^{A_8} \quad (1)$$

parameters A_0–A_8 were optimized with a simplex method based on the least average error

$$f_{min} = \sum_{j=1}^{18} \left[\frac{R_{0\,\exp j} - R_{0\,\mathrm{cal}\,j}}{R_{0\,\exp j}}\right]^2 \quad (2)$$

between the rates calculated from Eq. (1) and the experimental rates listed in Table 2. The following equation was found to be the best, which could represent the experimental data under all reaction conditions studied:

$$R_0 = 5.935 \times 10^{13} \exp(-7420/T) p_{H_2}^{0.573} p_{CO}^{0.625} C_{cat}^{0.225} \times C_{d1}^{0.296} W_{CTAB}^{2.202} \left(\frac{[P]}{[Rh]}\right)^{-0.532} \left(\frac{V_O}{V_W}\right)^{-1.437} \quad (3)$$

The comparison between the experimental and calculated rates is shown in Fig. 5 and the average deviation is 13.7%. The activation energy of hydroformylation reaction derived from Eq. (3) is 61.7 kJ mol^{-1}.

3.5. Effect of mass transfer

To ensure that the kinetic data were obtained under the conditions that mass transfer was not rate-limiting, the actual reaction rates were compared with the maximum rate of gas-to-liquid mass transfer. The gas–liquid mass transfer rate was calculated using the following empirical correlation obtained by oxidation of sodium sulfite solution in the same autoclave reactor (oxygen/*n*-decane/sodium sulfite solution with CTAB dispersion at 301 K) [12]

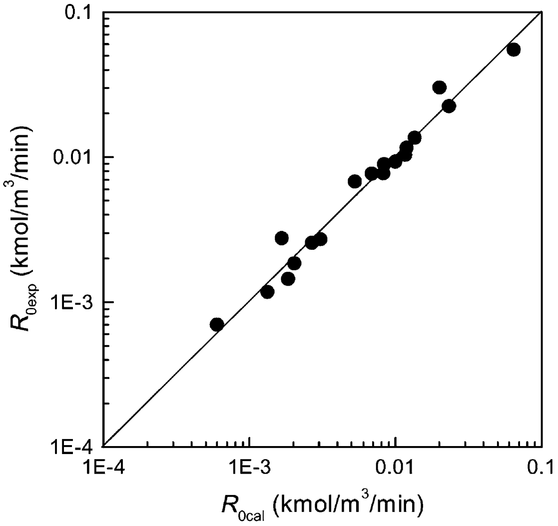

Fig. 5. Comparison of R_{0cal} calculated by Eq. (3) with R_{0exp}.

$$k_L a = 1.12 \times 10^{-11} n^{8.28} \left(\frac{H_1}{H_2}\right)^{0.93} \times \left(\frac{V_W}{V_O}\right)^{0.69} W_{CTAB}^{-1.56} \quad (4)$$

When the above correlation was used to evaluate the possible gas–liquid mass transfer resistance, the effects of gas properties and temperature on diffusivity were taken into account. Henry's law was used to evaluate the solubility of hydrogen and carbon monoxide necessary for the purpose of kinetic modeling. Neglecting the effect of gas film on gas–liquid–liquid mass transfer rate and ignoring the changes of liquid properties due to gas dissolution, the mass transfer in biphasic hydroformylation of 1-dodecene was analyzed. In doing this, the fact that the liquid–liquid dispersion system was composed of oil droplets in water for both the oxidation of sodium sulfite and the hydroformylation of 1-dodecene with the presence of CTAB was assured [13]. The following two cases are considered to shed light on the value of gas–liquid mass transfer coefficient.

Case 1. Chemical reaction in aqueous phase (oxidation of sodium sulfite)

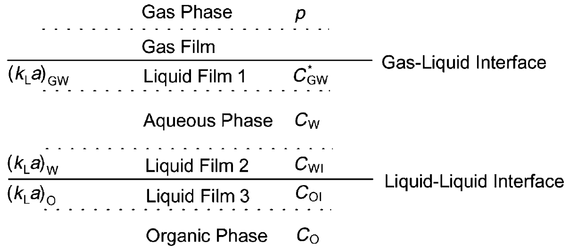

Fig. 6. Gas–liquid mass transfer for organic phase dispersed in aqueous phase.

The solubility of gas in water can be expressed as

$$C^*_{GW} = \frac{p}{H_W - p} C_{WS} \tag{5}$$

As sketched in Fig. 6, the mass transfer rate of gas to aqueous phase can be written as

$$\begin{aligned} N &= (k_La)^1_T(C^*_{GW} - C^1_W) \\ &= (k_La)^1_{GW}(C^*_{GW} - C^1_W) \end{aligned} \tag{6}$$

where the superscript 1 denotes Case 1, $(k_La)_{GW}$ denotes the measured mass transfer coefficient. Therefore

$$(k_La)^1_T = (k_La)_{GW} \tag{7}$$

namely, only the resistance related to one liquid film at the gas–liquid interface was measured in the oxidation of sodium sulfite.

Case 2. Chemical reaction at the organic–aqueous interface (biphasic hydroformylation of 1-dodecene)

The mass transfer rate of gas to liquid–liquid interface was

$$\begin{aligned} N &= (k_La)^2_T(C^*_{GW} - C^2_{WI}) = (k_La)_{GW}(C^*_{GW} - C^2_W) \\ &= (k_La)^2_W(C^2_W - C^2_{WI}) = R \end{aligned} \tag{8}$$

Under the condition that volumetric mass transfer coefficients for each liquid film, $(k_La)_{GW}$ and $(k_La)_W$, were equal, the following relation could be obtained:

$$(k_La)^2_T = \tfrac{1}{2}(k_La)_{GW} \tag{9}$$

Furthermore, combining Eqs. (7) and (9), the following equation is obtained:

$$(k_La)^2_T = \tfrac{1}{2}(k_La)^1_T \tag{10}$$

Considering that

$$(k_La)^2_T(C^*_{GW} - C^2_{WI}) = R$$

the actual concentration of dissolved gas at the aqueous side of the interface may be calculated by

$$C^2_{WI} = C^*_{GW} - \frac{2R}{(k_La)^1_T} \tag{11}$$

According to Henry's law, the equilibrium pressure of a gas component in the aqueous phase at liquid–liquid interface can be expressed as

$$p^{2*}_{WI} = \frac{C^2_{WI}}{C^2_{WI} + C_{WS}} H_W \tag{12}$$

By combining Eqs. (11) and (12), the following equation can be obtained:

$$p^{2*}_{WI} = \frac{C^*_{GW} - 2R/(k_La)^1_T}{C^*_{GW} - 2R/(k_La)^1_T + \rho_{WS}/M_{WS}} H_W \tag{13}$$

The calculated ratio of initial reaction rate to the maximum mass transfer rate of gas-to-liquid was presented in Table 5, which indicates that in some cases the mass transfer limitation is important to gas reactants, especially to carbon monoxide.

The effect of mass transfer rate of liquid-to-liquid on overall reaction rate is unimportant owing to very large liquid–liquid interfacial area in the presence of surfactant and intense stirring [13].

Table 5
Results of mass transfer analysis of macro-kinetics

Number	$R_0/(k_LaC^*_{H_2})$	$R_0/(k_LaC^*_{CO})$
1	0.0572	0.6347
2	0.0411	0.1303
3	0.1600	0.1191
4	0.0120	0.1355
5	0.2279	0.7188
6	0.0352	0.0256
7	0.0317	0.3486
8	0.0267	0.0830
9	0.1081	0.0793
10	0.0430	0.4690
11	0.0161	0.0509
12	0.1106	0.0807
13	0.0052	0.0560
14	0.0702	0.2197
15	0.2147	0.1587
16	0.0449	0.4936
17	0.0243	0.0756
18	0.1062	0.0779

3.6. Modified macro-kinetics

As mentioned above, the partial pressures of carbon monoxide and hydrogen do not directly represent the effects of dissolved gas concentration on reaction rates due to gas-to-liquid mass transfer resistance. More precisely, the kinetic equation should be correlated with the corrected gas partial pressure from Eq. (13). The modified kinetic equation is obtained as follows:

$$R_0 = 2.5485 \times 10^{17} \exp(-8533/T)(p^{*0.59}_{\mathrm{H}_2})(p^{*0.52}_{\mathrm{CO}}) \times C^{0.32}_{\mathrm{cat}} C^{0.41}_{\mathrm{d1}} W^{2.91}_{\mathrm{CTAB}} \left(\frac{[\mathrm{P}]}{[\mathrm{Rh}]}\right)^{-0.74} \left(\frac{V_\mathrm{O}}{V_\mathrm{W}}\right)^{-1.66} \quad (14)$$

As observed from Eq. (14), the reactant and catalyst concentrations are raised to fractional exponents, that is in accordance with Eq. (3). The activation energy calculated from Eq. (14) is 70.9 kJ mol^{-1}, which is higher than 61.7 kJ mol^{-1} obtained from Eq. (3). This means that the effect of temperature on reaction rate is more pronounced after the effect of mass transfer resistance on reaction rate is removed. This phenomenon is consistent with the principles of chemical reaction engineering that the effect of temperature on mass transfer rate may be depicted by an activation energy much lower than the intrinsic activation energy of a typical chemical reaction. Among other variables, W_{CTAB} and $V_\mathrm{O}/V_\mathrm{W}$ are the most important ones as suggested by their large values of exponent. A comparison of the experimental and predicted rates is presented in Fig. 7, and the average deviation between the predicted and experimental rates is 15.1%.

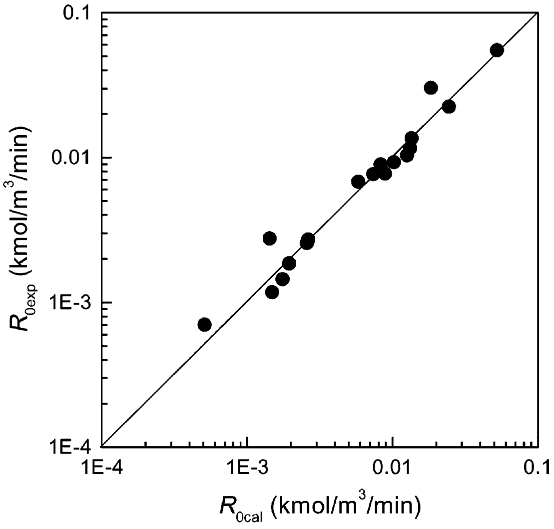

Fig. 7. Comparison of $R_{0\mathrm{cal}}$ calculated by Eq. (14) with $R_{0\mathrm{exp}}$.

3.7. Reaction mechanism and interfacial kinetics of biphasic hydroformylation

The mechanism of homogeneous hydroformylation as shown in Fig. 8 is widely accepted [14]. As for biphasic hydroformylation in the presence of a cationic surfactant, no report has been published. Larpent et al. [7] and Chen et al. [10] reported that the reaction of

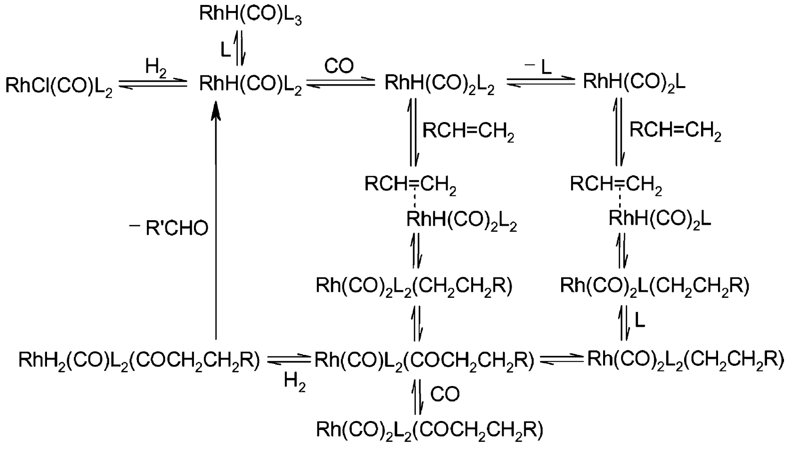

Fig. 8. Mechanism of homogeneous hydroformylation (L: PPh$_3$).

hydroformylation occurred mainly at the interface between organic and aqueous phases, for the cationic surfactant molecules enriched at the liquid–liquid interface could attract the water-soluble catalyst with negative charge to the interface by electrostatic attraction (as shown in Fig. 9). This results in effective contact between the water-insoluble higher olefins with the water-soluble catalyst and significant enhancement of reaction rate.

By combining the homogeneous catalytic mechanism with interfacial reaction, the biphasic hydroformylation mechanism is sketched in Fig. 10, where L and L′ denote TPPTS and cationic cetyl trimethyl ammonium (CTA) ions respectively. This mechanism is too complicated to derive a kinetic equation analytically. In addition, the chemical reaction equilibrium constants and reaction rate constants of intermediates are all unknown. A simplified mechanism sketch, as shown in Fig. 11, is attempted which contains the main reaction steps. The hydrogenolysis of intermediate 6 or the addition of olefin to produce acyl complex 6 is assumed as a rate-controlling step, other steps are fast reactions.

Case 1. Hydrogenolysis of intermediate 6 is the rate-limiting step [15].

Assumption is made that the starting intermediate species at the reaction interface is the complex

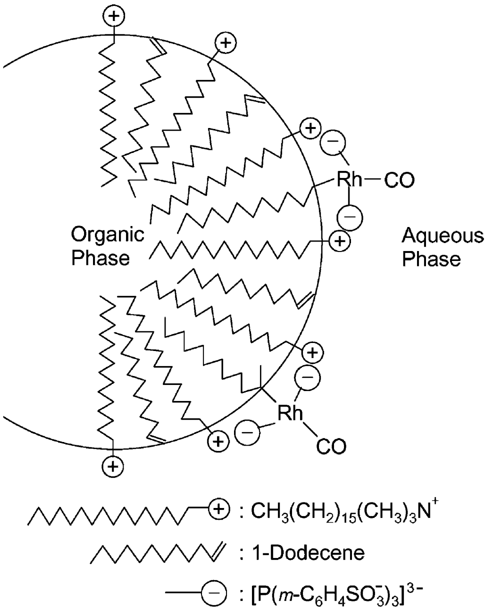

Fig. 9. Biphasic hydroformylation at liquid–liquid interface with CTAB for oil in water dispersion.

$HRh(CO)(TPPTS)_3$, the concentration of which is denoted by the term C_1. C_2–C_6 represent the concentrations of the intermediates labeled in Fig. 11, $HRh(CO)L_2$, $[L'][HRh(CO)L_2]$, $[L']_2[HRh(CO)L_2]$, $[L']_2[HRh(CO)_2L_2]$ and $[L']_2[Rh(CO)L_2(COCH_2$

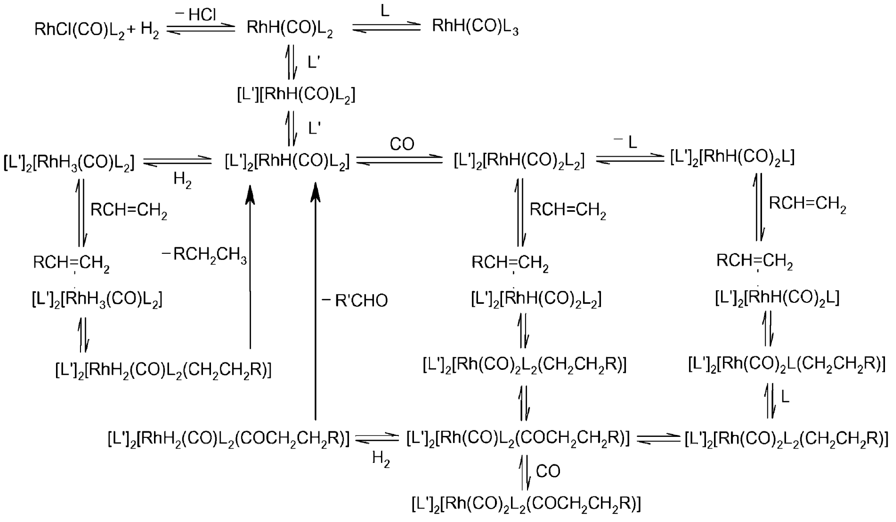

Fig. 10. Mechanism of biphasic hydroformylation (L: TPPTS; L′: CTA).

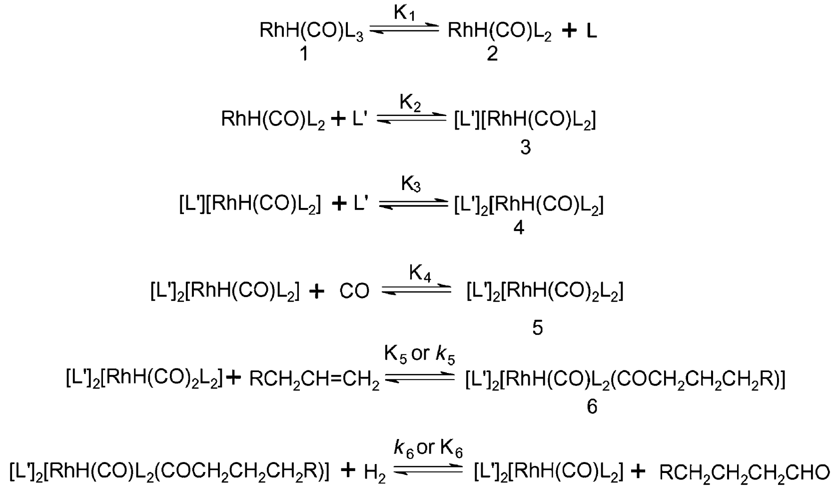

Fig. 11. Simplified mechanism of biphasic hydroformylation.

$CH_2CH_2R)$], respectively. Considering the pseudo-steady state of the reacting system, the rate of the reaction is given by

$$R = k_6 C_6 C_{H_2} \tag{15}$$

Considering the conservation of the catalytic species, the overall balance is described by

$$C_{cat} = C_1 + C_2 + C_3 + C_4 + C_5 + C_6 \tag{16}$$

where C_{cat} is the amount of catalyst loaded. The total concentrations of CTAB and TPPTS are also formulated as follows:

$$C_{CTAB,T} = C_{CTAB} + C_3 + 2C_4 + 2C_5 + 2C_6 \tag{17}$$

$$C_{L,T} = C_L + C_1 \tag{18}$$

The concentrations of C_1–C_5 can be expressed in terms of C_6, and hence C_{cat}, which are in turn substituted in Eq. (15) to give the rate model of the following form:

$$R = \frac{kC_{CTAB}^2 C_{d1} C_{CO} C_{cat} C_{H_2}}{1 + K_1^* C_L + K_2^* C_{CTAB} + K_3^* C_{CTAB}^2 + K_4^* C_{CTAB}^2 C_{CO} + K_5^* C_{CTAB}^2 C_{d1} C_{CO}} \tag{19}$$

where k and K_1^*–K_5^* are constants derived from the rate constant k_6 and equilibrium constants K_1–K_5 of elementary steps in the reaction mechanism in Fig. 11. The rate parameters to be determined were then optimized using all the experimental data. It was found that the data could not be fitted properly using Eq. (19).

Case 2. The formation of acyl complex 6 is the rate-controlling step [9].

The reaction rate is then given by

$$R = k_5 C_5 C_{d1} \tag{20}$$

Following the similar derivation, the final form of the rate model is

$$R = \frac{kC_{CTAB}^2 C_{CO} C_{cat} C_{H_2} C_{d1}}{(1 + K_1^* C_L + K_2^* C_{CTAB} + K_3^* C_{CTAB}^2 + K_4^* C_{CTAB}^2 C_{CO}) C_{H_2} + K_5^* C_{CTAB}^2} \tag{21}$$

where k and K_1^*–K_5^* are constants derived from the elementary equilibrium constants k_5, K_1–K_4 and K_6. This rate equation also gave very poor fitting results.

It is possible that the simplified mechanism is too simple to represent the real reaction mechanism. As indicated by the kinetic Eq. (14), the volume ratio of organic phase to aqueous phase is of great importance to the reaction rate, which may influence the liquid–liquid dispersion and liquid–liquid interfacial area, and hence the reaction rate. Therefore, this variable should be contained in the kinetic model. The effect of temperature on the rate coefficient is postulated as the usual Arrhenius equation:

$$k = A_0 \exp(A_1/T) \tag{22}$$

In view of the above results on mechanism analysis, several kinetic models could be proposed:

$$R = \frac{A_0 \exp(A_1/T)\, C_{\mathrm{CTAB}}^2 p_{\mathrm{H_2}} p_{\mathrm{CO}} C_{\mathrm{cat}} C_{\mathrm{d1}} (V_{\mathrm{O}}/V_{\mathrm{W}})^{A_8}}{(1 + A_2 C_{\mathrm{L}}/C_{\mathrm{cat}})(1 + A_3 \exp(A_9/T) p_{\mathrm{H_2}})(1 + A_4 p_{\mathrm{CO}})(1 + A_5 C_{\mathrm{cat}})(1 + A_6 W_{\mathrm{CTAB}})(1 + A_7 C_{\mathrm{d1}})} \tag{23}$$

$$R = \frac{A_0 \exp(A_1/T)\, C_{\mathrm{CTAB}}^2 p_{\mathrm{H_2}} p_{\mathrm{CO}} C_{\mathrm{cat}} C_{\mathrm{d1}} (V_{\mathrm{O}}/V_{\mathrm{W}})^{A_8}}{(1 + A_2 C_{\mathrm{L}}/C_{\mathrm{cat}})(1 + A_3 \exp(A_9/T)\, p_{\mathrm{H_2}})(1 + A_4 p_{\mathrm{CO}})(1 + A_5 C_{\mathrm{cat}})(1 + A_6 W_{\mathrm{CTAB}})(1 + A_7 C_{\mathrm{d1}})} \tag{24}$$

By the least square data-fitting, it is found that model (24) fits the data best after the parameters were optimized, which gives the following semi-empirical macro-kinetic equation:

$$R_0 = \frac{3.806 \times 10^{18} \exp(-8755/T) p_{\mathrm{H_2}} p_{\mathrm{CO}} C_{\mathrm{cat}} C_{\mathrm{d1}} W_{\mathrm{CTAB}}^2 (V_{\mathrm{O}}/V_{\mathrm{W}})^{-1.44}/(1 + 0.03423([\mathrm{P}]/[\mathrm{Rh}]))}{(1 + 2657 \exp(-2558/T)\, p_{\mathrm{H_2}})(1 + 1.672\, p_{\mathrm{CO}})(1 + 3307\, C_{\mathrm{cat}})(1 + 1.646\, C_{\mathrm{d1}})(1 - 44.26\, W_{\mathrm{CTAB}})} \tag{25}$$

This model indicates that the exponents of reactants (H_2, CO, 1-dodecene) are fractional for the initial reaction rate in accordance with the empirical kinetic equation. The activation energy derived from the model is 72.8 kJ mol^{-1} which is approximate to that obtained from Eq. (14), 70.9 kJ mol^{-1}. The comparison of predicted and experimental data is also reasonable (Fig. 12), and the average deviation of predictions is 14.1%.

Bhanage et al. [16] reported that the rate model of homogeneous hydroformylation of 1-dodecene catalyzed by $HRh(CO)(PPh_3)_3$ with an average deviation of 8%.

$$R = \frac{k C_{\mathrm{H_2}} C_{\mathrm{CO}} C_{\mathrm{cat}} C_{\mathrm{d1}}}{(1 + K_{\mathrm{CO}} C_{\mathrm{CO}})^2 (1 + K_{\mathrm{d1}} C_{\mathrm{d1}})} \tag{26}$$

The rate is first order to the concentrations of hydrogen and catalyst as that in Eq. (25). As for carbon monoxide and 1-dodecene, there exists typical substrate depression similar to Eq. (25). Also, the homogeneous activation energy is 57.1 kJ mol^{-1}, which is lower than that of biphasic hydroformylation with the hydrogenolysis of acyl complexes considered as the rate-controlling step.

Deshpande et al. [9] reported the kinetics of hydroformylation of 1-octene with ethanol as cosolvent:

$$R = \frac{k C_{\mathrm{H_2}} C_{\mathrm{CO}} C_{\mathrm{cat}} C_{\mathrm{C_8H_{16}}}}{(1 + K_{\mathrm{H_2}} C_{\mathrm{H_2}})(1 + K_{\mathrm{CO}} C_{\mathrm{CO}})^3} \tag{27}$$

which is similar to that of homogeneous hydroformylation.

However, in the presence of a cationic surfactant, the biphasic hydroformylation occurs at the liquid–liquid interface [7,10]. The surfactant has important influence on the mechanism, hence on the reaction rate. Furthermore, the liquid–liquid dispersion and interfacial area are also greatly influenced by the surfactant and impose effects on reaction rate. The differences between this biphasic kinetic equation and homogeneous one are ascribed to these factors. In view of these, more systematic experimental work and thorough analytical modeling of the reaction mechanism are desired.

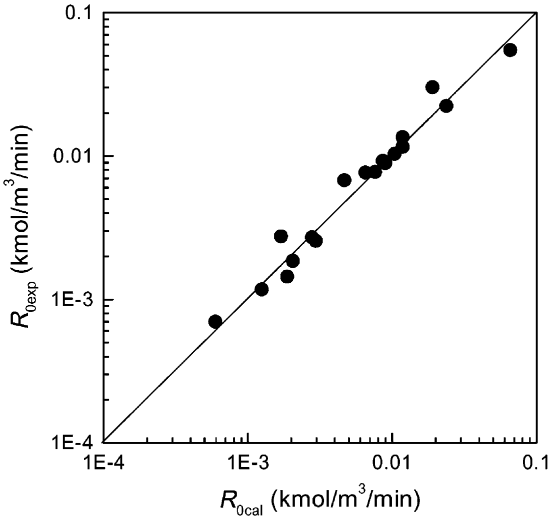

Fig. 12. Comparison of Eq. (25) with experimental data.

4. Conclusions

The macro-kinetics of biphasic hydroformylation of 1-dodecene catalyzed by water-soluble catalyst $RhCl(CO)(TPPTS)_2$ has been investigated in the presence of cationic surfactant CTAB. An orthogonal experimental design was adopted to study the effects of concentrations of reactants, catalyst, surfactant and ligand, temperature, the volume ratio of organic phase to aqueous phase on reaction rates. The optimal reaction conditions are suggested by the margin and variance analyses of experimental data according to the reaction rate with suitable compromise of the ratio of normal/isomeric aldehydes and hydroformylation selectivity to aldehyde. Besides, two new experimental facts related with the favorable role of large volume ratio of aqueous/organic phases and the correlation between the ratio of *n*/*i* aldehyde product and the rate of dodecene hydrogenation deserve further attention. The analysis of mass transfer resistance indicates the presence of mass transfer limitation under certain reaction conditions. Having corrected the effect of mass transfer, an empirical macro-kinetic equation is developed, which represents the experimental data rather well. By considering factors of biphasic mechanism, a semi-empirical kinetic model is proposed which is in good agreement with the experimental data.

Acknowledgements

We acknowledge gratefully the financial support from the National Natural Science Foundation of China (No. 29792074) and SINOPEC. We also thank Prof. Xianjun Li, Department of Chemistry, Sichuan University, China, for providing us the catalyst and ligand used in the present investigation.

References

[1] E.G. Kuntz, CHEMTECH 17 (1987) 570.

[2] E. Wiebus, B. Cornils, Hydrocarbon Process. 66 (1996) 63.

[3] J.Ch. Wu, G. Yuan, Q.Zh. Zhou, Shiyou Huagong (Petrochem. Ind.), 20 (1991), 79 (in Chinese).

[4] H. Chen, Y.Zh. Li, P.M. Cheng, Q. Yang, X.J. Li, Fenzi Cuihua (Mol. Catal.), 8 (1994) 347 (in Chinese).

[5] H. Bahrmann, P. Lappe, Eur. Patent Appl. EP602463 (1994).

[6] P. Purwanto, H. Delmas, Catal. Today 24 (1995) 135.

[7] C. Larpent, F. Brise LeMenn, H. Patin, New J. Chem. 15 (1991) 361.

[8] O. Wachsen, K. Himmler, B. Cornils, Catal. Today 42 (1998) 373.

[9] R.M. Deshpande, P. Purwanto, H. Delmas, R.V. Chaudhari, Ind. Eng. Chem. Res. 35 (1996) 3927.

[10] H. Chen, Y.Z. Li, J.R. Chen, P.M. Cheng, Y.E. He, X.J. Li, J. Mol. Catal. A 149 (1999) 1.

[11] H. Chen, H.Ch. Liu, Y.Zh. Li, P.M. Cheng, X.J. Li, Fenzi Cuihua (Mol. Catal.), 9 (1995) 145 (in Chinese).

[12] Y.Q. Zhang, Z.S. Mao, J.Y. Chen, Huagong Yejin (Eng. Chem. Metal.), 21 (2000), 123 (in Chinese).

[13] Y.Q. Zhang, Ph.D. Dissertation, Institute of Chemical Metallurgy, Chinese Academy of Sciences, Beijing, China, 1999 (in Chinese).

[14] D. Evans, A. Osborn, G. Wilkinson, J. Chem. Soc. A (12) (1968) 3133.

[15] Y.Zh. Yuan, Y.Q. Yang, J.L. Xu, H.B. Zhang, K.R. Tsai, Chin. Chem. Lett. 5 (1994) 291.

[16] B.M. Bhanage, S.S. Divekar, R.M. Deshpande, R.V. Chaudhari, J. Mol. Catal. A 115 (1997) 247.